

Absolute cross sections for deuteron-induced reactions on ${}^6\text{Li}$ at energies below 1 MeV[†]

A. J. Elwyn, R. E. Holland, C. N. Davids, L. Meyer-Schutzmeister, J. E. Monahan, F. P. Mooring,
and W. Ray, Jr.

Argonne National Laboratory, Argonne, Illinois 60439

(Received 22 July 1977)

Absolute cross sections for (d, n) , (d, p) , and (d, α) reactions initiated by ~ 0.1 to ~ 1.0 MeV deuterons on ${}^6\text{Li}$ have been obtained. Total reaction cross sections, with absolute accuracies of 8–13%, as well as measured differential cross sections are presented. The experimental procedures are discussed and a comparison with previous results is given.

[NUCLEAR REACTIONS ${}^6\text{Li}(d, p)$, (d, α) , $E_d = 0.1\text{--}\sim 1.0$ MeV; ${}^6\text{Li}(d, n)$, $E_d = 0.2\text{--}\sim 0.9$ MeV; enriched target; measured $\sigma(E_d, \theta)$, $\sigma(E_d)$.]

I. INTRODUCTION

The main objective of the experimental study reported here is the accurate determination of both total and differential reaction cross sections for the various outgoing channels in deuteron-induced reactions on ${}^6\text{Li}$ at energies from ~ 100 keV up to ~ 1 MeV. Along with measurements, in the same energy range, of the elastic scattering of deuterons by ${}^6\text{Li}$, currently in progress, the work constitutes a complete study of all nuclear reactions initiated by low-energy deuterons on ${}^6\text{Li}$. This research effort is part of a more general program to measure absolute reaction cross sections for various light ions with light nuclei at energies below a few MeV.

The motivation behind these studies is twofold. In the first place, reaction cross-section data are important to the understanding of the nuclear structure of light elements and of the underlying reaction mechanisms. Although reactions of light ions with light nuclei constitute some of the earliest studies undertaken with particle accelerators, many of the previous results represent only partial and, in some cases, conflicting determinations of the cross sections relevant to such investigations.

Second, nuclear reactions that involve light nuclei are of interest¹ in the development of "advanced" fusion fuels. Of particular relevance in this connection are the cross sections in various light-ion-induced reactions on ${}^6\text{Li}$. Furthermore, thermonuclear reaction rates based on measured reaction cross sections are useful to studies of astrophysical interest.²

Table I lists the Q values for the various exothermic reactions of deuterons with ${}^6\text{Li}$. Discrepancies between different sets of measurements and gaps in the data exist in the previously reported

results for many of these processes at energies below 1 MeV. For reactions in which protons are emitted, Bertrand, Greiner, and Poiret,³ Bruno *et al.*,⁴ and McClenahan and Segel⁵ have published total reaction cross sections for both the ground- and first-excited state in the ${}^6\text{Li}(d, p){}^7\text{Li}$ reaction at energies down to 0.3 MeV, while Sawyer and Phillips,⁶ and Whaling and Bonner⁷ present data down to 30 keV at a single angle only. Macklin and Banta⁸ report cross sections for total tritium production in the ${}^7\text{Li}$ breakup process (i.e., $d + {}^6\text{Li} \rightarrow p + t + \alpha$) down to 380 keV.

The ${}^6\text{Li}(d, \alpha)\alpha$ reaction has been studied more extensively, although considerable disagreement exists between the various reported low-energy absolute measurements. Total reaction cross sections at energies less than a few MeV have been presented by Lee,⁹ Bertrand *et al.*,³ Bruno *et al.*,⁴ Jeronymo *et al.*,¹⁰ and McClenahan and Segal,⁵ while Sawyer and Phillips,⁶ Whaling and Bonner,⁷ and Hirst, Johnstone, and Poole¹¹ give 90° differential cross sections only.

For outgoing neutrons, Hirst *et al.*¹¹ report total reaction cross sections for both of the neutron groups together in the ${}^6\text{Li}(d, n){}^7\text{Be}$ reaction, while

TABLE I. Exothermic reactions of deuterons with ${}^6\text{Li}$.

Reaction	Q value (MeV)
${}^6\text{Li}(d, n_0){}^7\text{Be}$	3.38
${}^6\text{Li}(d, n_1){}^7\text{Be}^*(0.430 \text{ MeV})$	2.95
${}^6\text{Li} + d \rightarrow n + {}^3\text{He} + \alpha$	1.80
${}^6\text{Li}(d, p_0){}^7\text{Li}$	5.03
${}^6\text{Li}(d, p_1){}^7\text{Li}^*(0.478 \text{ MeV})$	4.55
${}^6\text{Li} + d \rightarrow p + t + \alpha$	2.56
${}^6\text{Li}(d, \alpha)\alpha$	22.38

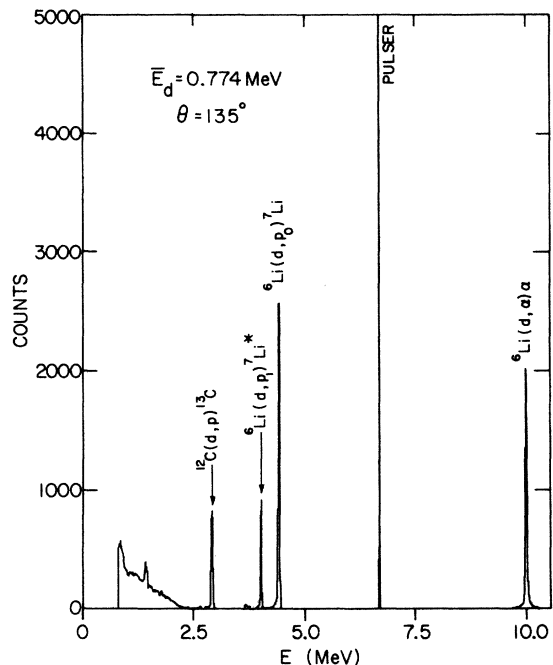


FIG. 1. Typical pulse-height spectrum of the charged particles that result in reactions of deuterons with targets of ${}^6\text{LiF}$ on carbon backings.

McClenahan and Segel⁵ in a more recent publication present results for the individual groups at somewhat higher energies. A preliminary report of the current Argonne measurements for the outgoing neutron channels has been presented previously.¹²

The present paper describes the results of measurements of both total and differential cross sections of the protons in the ${}^6\text{Li}(d,p){}^7\text{Li}$ reaction and the α particles in the ${}^6\text{Li}(d,\alpha)\alpha$ reaction at energies between ~ 0.1 and ~ 1.0 MeV, and neutrons in the ${}^6\text{Li}(d,n){}^7\text{Be}$ reaction from ~ 0.2 to ~ 0.9 MeV. The experiment in which the charged particles are detected is described in some detail in Sec. II. (A short description has previously been presented in Ref. 12.) A brief summary of the experimental procedure relevant to the neutron data is also given in Sec. II. Both the neutron and charged-particle results are discussed in Sec. III, and tables of measured cross sections are given in an Appendix. Measurements of the continuum protons and neutrons that arise in the ${}^7\text{Li}$ and ${}^7\text{Be}$ breakup reactions, respectively, are completed, and will be discussed in a separate publication.¹³ Tables giving thermonuclear reaction-rate and reactivity parameters, useful to the evaluation of ${}^6\text{Li}$ as a fusion fuel, calculated from the measured reaction cross sections shown here have been published.¹⁴

II. EXPERIMENT

The emphasis in these measurements was on the determination of absolute reaction cross sections in the low-energy region to accuracies of $\sim 10\%$. To this end considerable care was exercised to measure Li target thicknesses and total integrated charge accurately and reproducibly.

The experiment was performed at the Argonne 4-MV Dynamitron accelerator. The ${}^2\text{H}_3^+$ molecular ion beam rather than the ${}^2\text{H}_1^+$ ion was utilized since this made it possible to attain low deuteron energy on target ($\frac{1}{3}$ of the terminal voltage) at the higher terminal voltages at which more stable Dynamitron operating conditions prevailed. The ion beam, defined by two apertures placed about 25 cm apart, entered into a 76-cm diam scattering chamber. The targets, placed at the center of the chamber, were thin films ($75\text{--}100 \mu\text{g}/\text{cm}^2$) of LiF enriched to 99.3% in ${}^6\text{Li}$ evaporated onto thin ($10\text{--}15 \mu\text{g}/\text{cm}^2$) carbon foils. The use of LiF rather

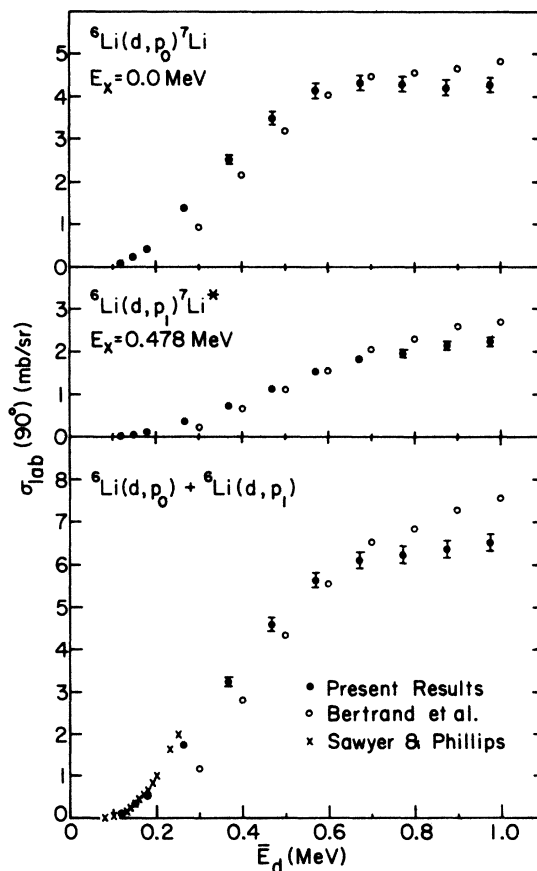


FIG. 2. Differential cross section at 90° (lab) for the ${}^6\text{Li}(d,p)$ reactions as a function of average lab deuteron energy, \bar{E}_d . The previous results shown here refer to Refs. 3 and 6 in text.

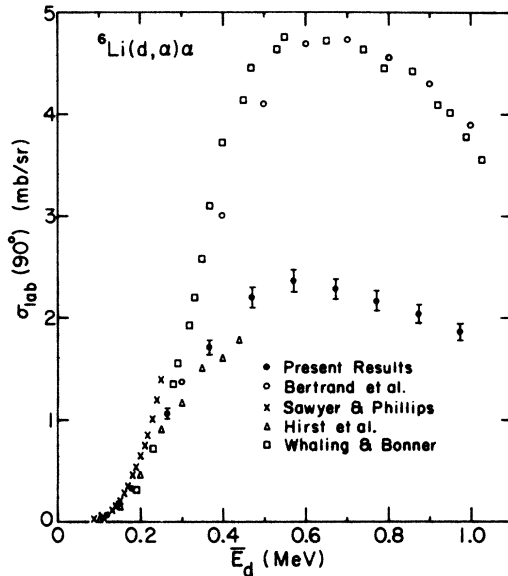


FIG. 3. Differential cross section at 90° (lab) for the ${}^6\text{Li}(d, \alpha)$ reaction as a function of average deuteron energy, \bar{E}_d . The previous results shown here refer to Refs. 3, 6, 7, and 11 in text.

than metallic lithium (which was possible because the nuclear-reaction yields from deuterons on fluorine are small at energies below 1 MeV) allowed the fabrication of very uniform and stable films of known composition. A beam current passing through the thin targets was collected in a Faraday cup, insulated from and attached to the back of the chamber, and the total charge was measured with a current integrator. The operation of this instrument was checked by use of batteries and precision resistors, and was always found to be accurate to better than 0.5%. No measurable effect on reaction product yield per unit integrated charge, due to secondary electron loss from the Faraday cup, was observed.

Charged particles in the reaction were detected by Si surface-barrier detectors thick enough to completely stop the reaction products. Two detectors were mounted on movable arms within the chamber, while a third, set at a fixed angle, served as a monitor in the angular distribution measurements. The solid angles of the two movable detectors, defined by rectangular or circular collimators placed in front of the detectors, varied from about 3×10^{-4} to 3×10^{-5} sr. The detectors were attached to low-noise preamplifiers. The pulses from the detector-preamp system were passed through spectroscopy amplifiers into 1024-channel analog-to-digital converters (ADC's) interfaced to an ASI-2100 computer, and the data were

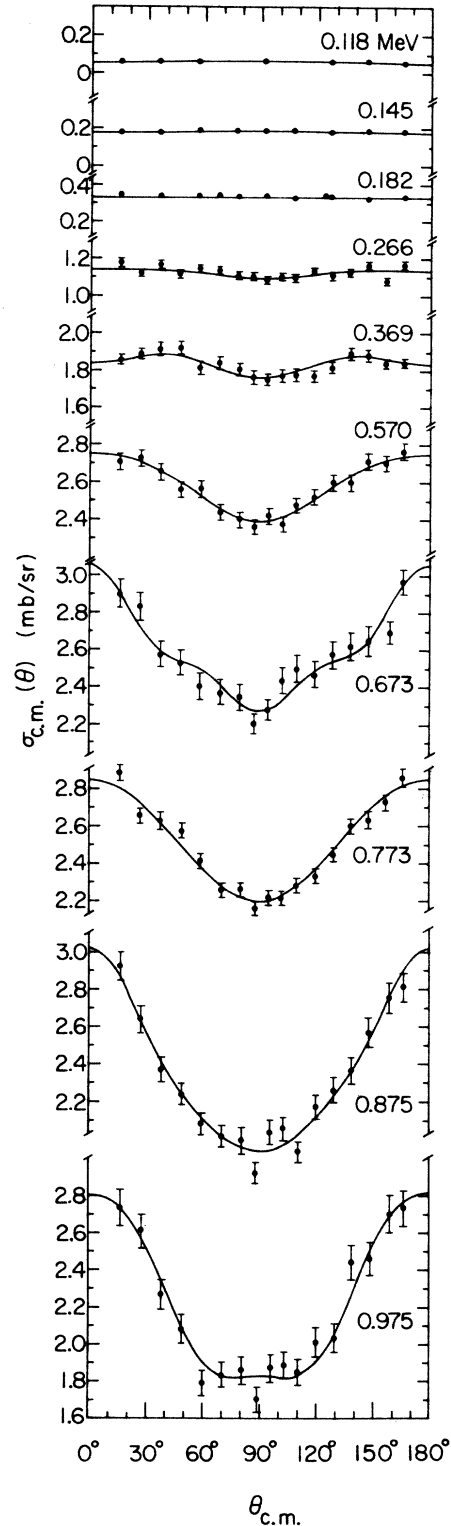


FIG. 4. Angular distributions of the α particles in the ${}^6\text{Li}(d, \alpha)$ reaction at the average deuteron energies indicated. The smooth curve at each energy represent the results of the Legendre polynomial fit.

TABLE II. Sources of uncertainties in total reaction cross-section measurements.

Source	Estimated uncertainty (%)		
	(d, p_0)	(d, p_1)	(d, α)
Counting statistics, peak area determination, etc.	3-5.5	4-11	4-5.5
Charge collection, target stability	3	3	3
Average deuteron energy	0.3-3	0.3-3	0.3-3
Total relative error	4.5-7	5-12	5-7
Target thickness, solid angle	7	7	7
Total absolute error	8-10	8.5-14	8.5-10

stored on magnetic tape. A typical pulse-height spectrum of the charged particles that result in reactions of deuterons with targets of ${}^6\text{LiF}$ on carbon backings is shown in Fig. 1.

The thickness of the targets was determined by two different techniques. In the first method, Rutherford scattering of alpha particles was used. The yield per unit integrated charge of 1-MeV α particles scattered from F (in the ${}^6\text{LiF}$ films) was measured at a number of angles between 25° and 60° . After verifying that the scattering was pure Rutherford at these laboratory angles, and correcting the yields for effective charge collection (see below), the thickness of the ${}^6\text{LiF}$ targets could be easily found. In the second method, the difference in energy for deuterons scattered at back angles (145° - 157.5°) from two thin layers of Au sandwiched around the ${}^6\text{LiF}$ deposit was determined. This energy difference is directly related to the energy loss of the deuterons in the LiF layer, and from tabulated atomic stopping powers¹⁵ the target thickness could be obtained. Although the method based on Rutherford scattering is inherently more precise (since tabulated stopping powers

necessary for the second technique may only be accurate to $\sim 10\%$ in many cases), target thickness determined in both ways agreed to $\pm 5\%$ which is within the absolute uncertainties of either method alone.

Relative angular distributions for the ground- and first-excited state protons in the ${}^6\text{Li}(d, p)$ reaction and the energetic α particles in the ${}^6\text{Li}(d, \alpha)$ process were obtained at angles from 15° to 165° for deuteron energies between 0.1 and 1.0 MeV from the yields measured in the two movable Si detectors relative to those in the fixed monitor detector. These yields, corrected for background and small electronic dead time effects, were divided by the values at 90° , and absolute differential cross sections were obtained by normalizing to separately measured 90° -excitation functions for each particle group. These latter 90° yields were measured relative to total integrated charge so that corrections had to be made for effective charge collection, since the amount of collected charge changes with the energy of the projectile. This arises because the charge state of the low-energy deuteron beam may be altered upon passage through the thin

TABLE III. The coefficients (in the c.m. system) in the expansion of the differential cross sections in a series of Legendre polynomials for the ${}^6\text{Li}(d, \alpha)\alpha$ reaction. The errors shown are based only on statistics and uncertainties in the fitting procedures.

\bar{E}_d (MeV)	B_0	B_2	B_4	B_6
	(mb/sr)			
0.118	0.063 ± 0.001	-0.005 ± 0.002		
0.145	0.161 ± 0.001	-0.004 ± 0.002		
0.182	0.336 ± 0.001	0.0 ± 0.002		
0.266	1.11 ± 0.01	0.03 ± 0.01	-0.02 ± 0.02	
0.369	1.79 ± 0.01	0.08 ± 0.01	-0.07 ± 0.02	
0.570	2.49 ± 0.01	0.25 ± 0.02	-0.04 ± 0.02	
0.673	2.51 ± 0.02	0.39 ± 0.04	0.03 ± 0.05	0.15 ± 0.07
0.773	2.38 ± 0.02	0.42 ± 0.03	0.03 ± 0.03	0.01 ± 0.05
0.875	2.21 ± 0.02	0.62 ± 0.04	0.14 ± 0.06	0.06 ± 0.08
0.975	2.08 ± 0.02	0.68 ± 0.04	0.17 ± 0.06	-0.10 ± 0.07

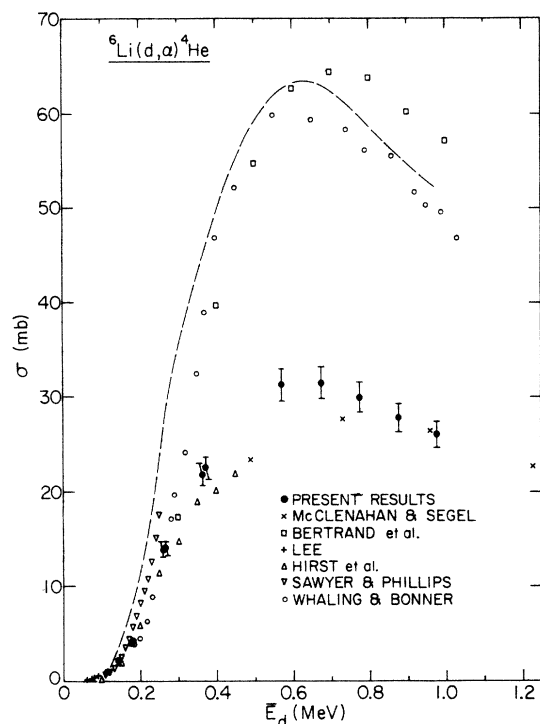


FIG. 5. Total reaction cross sections in the ${}^6\text{Li}(d, \alpha)$ reaction as a function of average deuteron energy, \bar{E}_d . The previous results shown here refer to Refs. 3, 5, 6, 7, 9, and 11 in the text. For Refs. 6, 7, and 11, $\sigma = 4\pi\sigma_{c.m.}(90^\circ)$. The relative precision of the present results is indicated by the error bars. The dashed curve represents *twice* the measured reaction cross sections obtained in the present experiment. (See text.)

${}^6\text{LiF}$ -plus-C films and because a portion of the beam could be scattered out of the solid angle of the Faraday cup by small-angle multiple scattering in the targets. The magnitude of these effects was determined at each energy by accurately measuring the ratio of the times necessary to integrate a steady beam current to a predetermined charge value with and without the target in place. The total integrated charge obtained in the 90° -excitation function measurements were then multiplied by these ratios at each incident deuteron energy to get the corrected values.

The 90° -excitation functions for the ${}^6\text{Li}(d, p_0)$, ${}^6\text{Li}(d, p_1)$, and ${}^6\text{Li}(d, \alpha)$ reactions are shown in Figs. 2 and 3, compared with previous measurements. (The large discrepancies, observed in Fig. 3, between the present results and some of the previous measurements are discussed in Sec. III in connection with Fig. 5.) The energy scales on these (and all subsequent relevant figures) represent average deuteron energies \bar{E}_d , which differ from the incident energy because of energy

loss in the ${}^6\text{LiF}$ targets. The average deuteron energy, defined as that energy at which the measured cross section is equal to the "true" cross section, was determined in the following manner: The true cross section at the energy \bar{E}_d , $\sigma(\bar{E}_d)$, was set equal to the measured cross section, viz,

$$\int_0^t \frac{dE}{dx} \sigma(E) dx / \int_0^t \frac{dE}{dx} dx,$$

where t is the target thickness and dE/dx is the

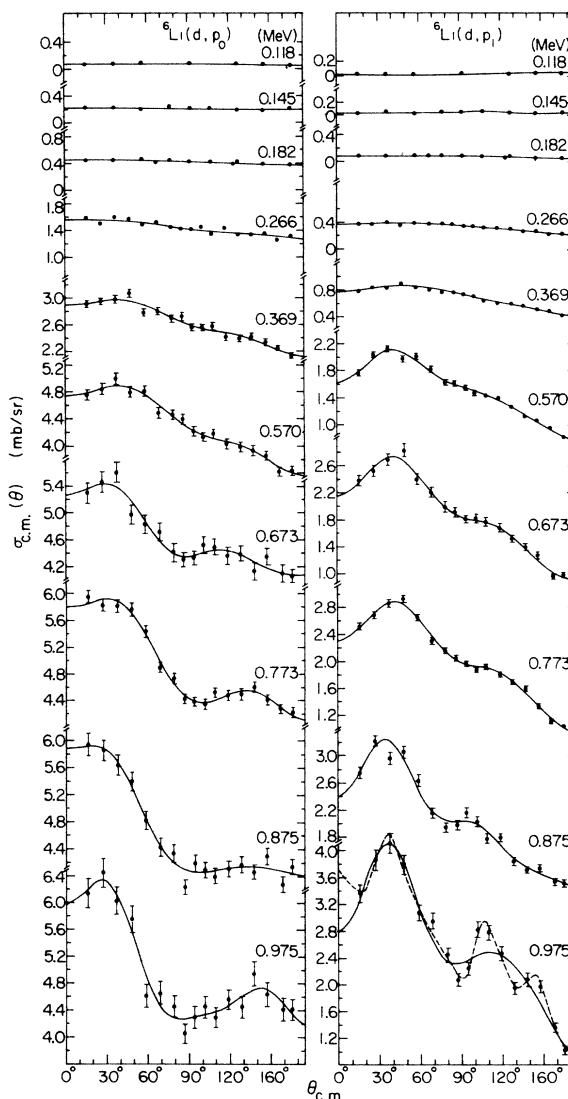


FIG. 6. Angular distributions of the protons in the ${}^6\text{Li}(d, p)$ reactions at the average deuteron energies indicated. The smooth curve at each energy represent the results of the Legendre polynomial fit. At 0.975 MeV in the ${}^6\text{Li}(d, p_1)$ process, the solid curve is a 7 polynomial fit while the dashed curve represents a fit to 11 polynomials.

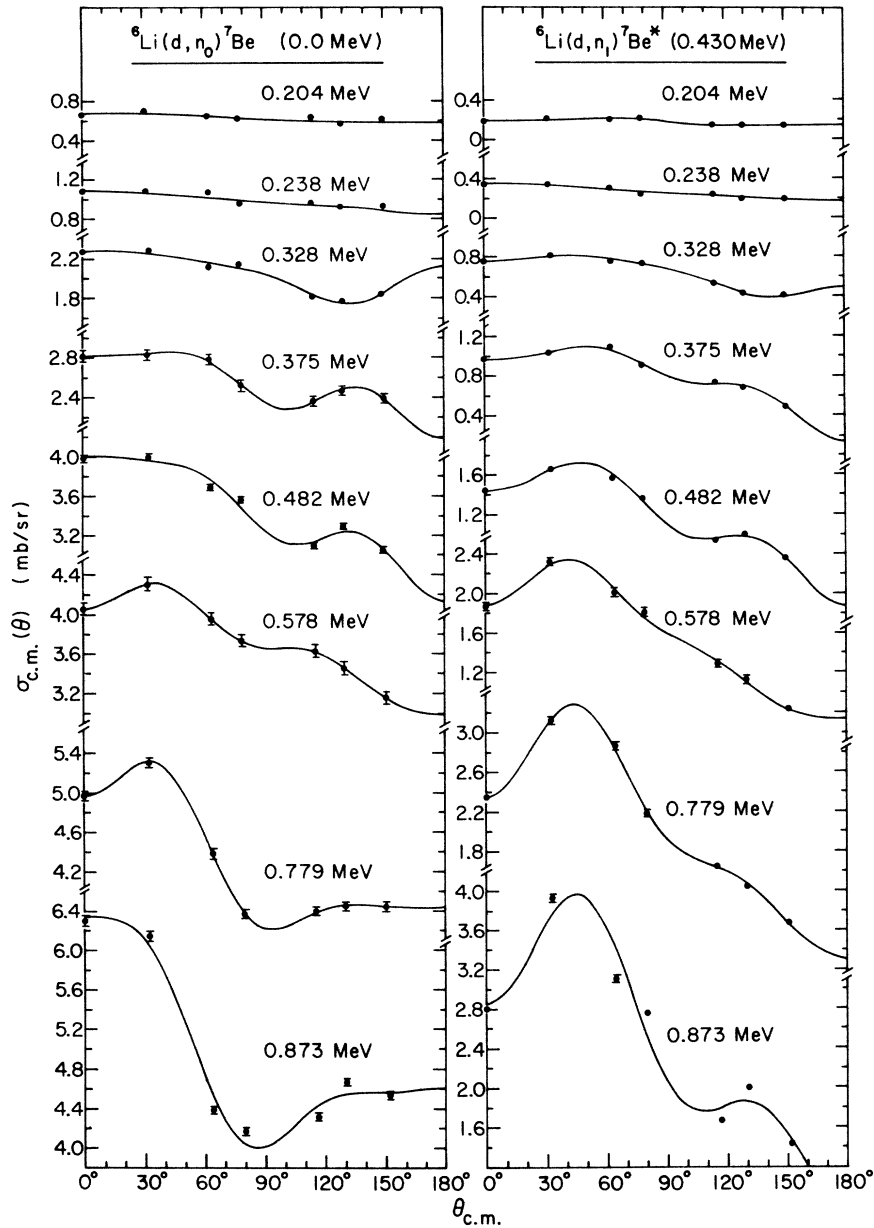


Fig. 7. Angular distributions of the neutrons in the ${}^6\text{Li}(d, n)$ reactions at the average deuteron energies indicated. The smooth curves at each energy represent the results of the Legendre polynomial fit.

atomic stopping power of ${}^6\text{LiF}$. In this expression the energy dependence of the stopping power was assumed to be linear over the target thickness, while that of the $d + {}^6\text{Li}$ reaction cross-section $\sigma(E)$ was represented by the approximate low-energy extrapolation, $P_0(E)/E$, where $P_0(E)$ is the s -wave penetrability at relative energy E (in the c.m. system) of the deuteron and ${}^6\text{Li}$ in the incident channel. For a given target thickness ($75\text{--}100 \mu\text{g}/\text{cm}^2$) values of \bar{E}_d appropriate to the $d + {}^6\text{Li}$ reactions at in-

cident energies E_d between 0.1 and 1.0 MeV were determined by evaluating the above expression numerically.¹⁶ The results indicate that except at incident energies below $\sim 250 \text{ keV}$, $\bar{E}_d \approx E_d - \frac{1}{2} \Delta$, where Δ is the target thickness in energy units determined from tabulated atomic stopping powers at the incident energy E_d . For $E_d < 250 \text{ keV}$, \bar{E}_d is from 2 to 6 keV larger than would be predicted by the expression $\bar{E}_d = E_d - \frac{1}{2} \Delta$.

The beam line and target chamber system were

pumped by liquid-nitrogen trapped oil diffusion and turbomolecular pumps and by a liquid-nitrogen cooled sorption trap to typical chamber pressures of less than 10^{-6} Torr. In addition, the beam (generally 10–100 nA) entering the chamber passed through an inline liquid-nitrogen cold finger. For the most part, therefore, carbon contaminant buildup on the ${}^6\text{LiF}$ targets, which was monitored by measuring the yield of protons in the ${}^{12}\text{C}(d,p)$ ${}^{13}\text{C}$ reaction at a given incident energy at frequent intervals, was kept to a minimum. Even so, some carbon did build up on the face of the targets, and this necessitated target replacement from time to time, particularly for low incident energies at which cross sections vary rapidly with energy. Corrections to the average energy due to carbon buildup was estimated to be about 1–2 keV during the time required to perform a complete angular distribution, and although this correction was not actually made, estimates of the errors in the cross-section measurements did take these effects into account.

The total reaction cross section at each energy was obtained from the expansion of the measured differential cross sections in a series of Legendre polynomials. Absolute uncertainties in these values are estimated to be between 8 and 13% throughout. Table II lists the sources of the estimated uncertainties in the total cross-section measurements. The first line represents the errors associated with the yield determination in the angular distribution and 90° -excitation function measurements. In addition, it also includes uncertainties in the results of the Legendre polynomial fitting. The errors associated with charge collection include uncertainties in the measurement of the correction factors for effective charge determination and long-term target stability, while the values shown under average deuteron energy include errors in target thickness, machine energy, and carbon buildup. The target thickness uncertainties include errors in the Rutherford scattering cross section that arise from uncertainties in the angles¹⁷ at which the measurements were performed, as well as counting statistics and errors in the machine energy.

As mentioned, the description of the experiment relevant to the determination of cross sections in the ${}^6\text{Li}(d,n){}^7\text{Be}$ reactions has been reported¹² in some detail. For completeness, however, a brief summary is included here. Neutron yields were obtained at four angles simultaneously by time-of-flight techniques using the pulsed and bunched Dynamitron beam. The detectors were cylindrical stilbene scintillators, 2.54 cm long by 5.08 cm in diameter, directly coupled to RCA-8575 photo-multipliers. With flight paths of ~ 3.5 m the neu-

TABLE IV. The coefficients (in the c.m. system) in the expansion of the differential cross sections in a series of Legendre polynomials for the ${}^6\text{Li}(d,p){}^7\text{Li}$ reactions. The errors shown are based only on statistics and uncertainties in the fitting procedure.

Reaction	\bar{E}_d (MeV)	B_0	B_1	B_2	B_3 (mb/sr)	B_4	B_5	B_6	B_7	B_8	B_9	B_{10}
(d,p_0)	0.118	0.075 ± 0.002	0.005 ± 0.002	-0.008 ± 0.003								
	0.145	0.190 ± 0.004	0.017 ± 0.006	-0.008 ± 0.007								
	0.182	0.424 ± 0.004	0.042 ± 0.006	-0.011 ± 0.007								
	0.266	1.417 ± 0.009	0.14 ± 0.02	0.004 ± 0.02								
	0.369	2.59 ± 0.01	0.39 ± 0.02	-0.02 ± 0.03	-0.01 ± 0.03	-0.12 ± 0.04						
	0.570	4.25 ± 0.02	0.64 ± 0.03	-0.01 ± 0.03	-0.04 ± 0.04	-0.19 ± 0.05						
	0.673	4.62 ± 0.03	0.61 ± 0.05	0.32 ± 0.06	0.21 ± 0.08	-0.24 ± 0.08	-0.22 ± 0.10					
	0.773	4.67 ± 0.04	0.85 ± 0.05	0.46 ± 0.06	0.18 ± 0.9	-0.28 ± 0.09	-0.06 ± 0.10					
	0.875	4.51 ± 0.05	0.89 ± 0.08	0.73 ± 0.09	0.21 ± 0.12	-0.23 ± 0.13	-0.15 ± 0.15	-0.07 ± 0.16				
	0.975	4.80 ± 0.05	0.74 ± 0.08	0.96 ± 0.10	0.39 ± 0.12	-0.35 ± 0.14	-0.21 ± 0.17	-0.33 ± 0.18				
(d,p_1)	0.118	0.015 ± 0.001	0.002 ± 0.001	-0.001 ± 0.001								
	0.145	0.042 ± 0.002	0.006 ± 0.003	-0.005 ± 0.004								
	0.182	0.094 ± 0.001	0.015 ± 0.002	-0.013 ± 0.002	-0.003 ± 0.002	-0.001 ± 0.003						
	0.266	0.342 ± 0.003	0.069 ± 0.005	-0.041 ± 0.006	0.0 ± 0.008	-0.007 ± 0.009						
	0.369	0.70 ± 0.01	0.20 ± 0.01	-0.07 ± 0.01	-0.03 ± 0.01	-0.05 ± 0.01						
	0.570	1.55 ± 0.01	0.56 ± 0.02	-0.11 ± 0.02	-0.03 ± 0.03	-0.21 ± 0.03	-0.12 ± 0.03					
	0.673	1.95 ± 0.02	0.82 ± 0.03	-0.07 ± 0.04	0.0 ± 0.05	-0.36 ± 0.05	-0.18 ± 0.07	0.0 ± 0.07				
	0.773	2.10 ± 0.03	0.91 ± 0.04	-0.05 ± 0.04	-0.02 ± 0.05	-0.35 ± 0.05	-0.13 ± 0.07	-0.04 ± 0.06				
	0.875	2.09 ± 0.03	0.98 ± 0.05	0.08 ± 0.06	0.13 ± 0.09	-0.21 ± 0.10	-0.43 ± 0.11	-0.24 ± 0.12				
	0.975	2.69 ± 0.02	1.10 ± 0.04	0.17 ± 0.05	0.38 ± 0.06	-0.65 ± 0.07	-0.49 ± 0.08	-0.06 ± 0.08	0.27 ± 0.10	-0.44 ± 0.11	0.12 ± 0.11	0.66 ± 0.11

TABLE V. The coefficients (in the c.m. system) in the expansion of the differential cross sections in a series of Legendre polynomials for the ${}^6\text{Li}(d, n){}^7\text{Be}$ reactions. The errors shown are based only on statistics and uncertainties in the fitting procedure.

Reaction	\bar{E}_d	B_0	B_1	B_2	B_3	B_4	B_5
(d, n_0)	0.204	0.63 ± 0.01	0.05 ± 0.02	0.01 ± 0.02			
	0.238	0.98 ± 0.02	0.09 ± 0.02	0.03 ± 0.03			
	0.328	2.02 ± 0.04	0.27 ± 0.05	0.05 ± 0.07	-0.13 ± 0.07	0.13 ± 0.14	-0.06 ± 0.11
	0.375	2.53 ± 0.02	0.32 ± 0.02	0.14 ± 0.03	-0.05 ± 0.03	0.27 ± 0.06	0.15 ± 0.05
	0.482	3.43 ± 0.07	0.58 ± 0.11	0.13 ± 0.14	-0.03 ± 0.15	-0.29 ± 0.27	0.19 ± 0.23
	0.578	3.744 ± 0.001	0.571 ± 0.001	-0.013 ± 0.002	0.117 ± 0.002	-0.209 ± 0.004	-0.153 ± 0.003
	0.779	4.15 ± 0.02	0.79 ± 0.03	0.70 ± 0.04	0.0 ± 0.04	-0.45 ± 0.07	-0.23 ± 0.06
	0.873	4.66 ± 0.13	0.68 ± 0.20	1.09 ± 0.27	0.43 ± 0.27	-0.28 ± 0.48	-0.24 ± 0.45
(d, n_1)	0.204	0.177 ± 0.005	0.05 ± 0.01	-0.01 ± 0.01	-0.03 ± 0.01		
	0.238	0.26 ± 0.01	0.08 ± 0.01	0.01 ± 0.02	0.01 ± 0.02		
	0.328	0.65 ± 0.01	0.24 ± 0.01	-0.06 ± 0.01	-0.06 ± 0.01	0.04 ± 0.02	-0.05 ± 0.02
	0.375	0.84 ± 0.02	0.34 ± 0.03	-0.10 ± 0.04	-0.01 ± 0.04	-0.18 ± 0.08	0.08 ± 0.07
	0.482	1.22 ± 0.03	0.57 ± 0.05	-0.04 ± 0.06	-0.11 ± 0.06	-0.32 ± 0.12	0.12 ± 0.10
	0.578	1.62 ± 0.04	0.82 ± 0.06	-0.11 ± 0.08	-0.10 ± 0.08	-0.20 ± 0.15	-0.15 ± 0.13
	0.779	2.12 ± 0.04	1.20 ± 0.06	-0.04 ± 0.08	-0.24 ± 0.03	-0.56 ± 0.14	-0.14 ± 0.12
	0.873	2.49 ± 0.21	1.41 ± 0.31	0.21 ± 0.41	-0.42 ± 0.38	-0.86 ± 0.72	0.02 ± 0.67

tron groups corresponding to the ground- and first-excited states in ${}^7\text{Be}$ could be resolved. Absolute differential cross sections were obtained from the measured yields, after correction for background effects, by use of absolute detector efficiencies determined in a separate measurement of the neutron yields in the ${}^7\text{Li}(p, n){}^7\text{Be}$ and ${}^2\text{H}(d, n){}^3\text{He}$ reactions. (See Ref. 12 for further details. In particular, the cross sections used to determine absolute detector efficiencies are from Refs. 6 and 7 cited in Ref. 12.) Results were obtained at seven angles for deuteron energies between 0.204 and 0.880 MeV. Absolute total reaction cross sections extracted from the measured angular distributions have estimated uncertainties of 13–16%.

III. RESULTS AND DISCUSSION

The angular distributions of the α particles in the ${}^6\text{Li}(d, \alpha)\alpha$ reaction are shown in Fig. 4. The smooth curves are the results of the Legendre polynomial fits. Since the angular distribution must be symmetric about 90° in the center of mass, the fit includes only even-order polynomials, the values of which are given in Table III. When odd-order polynomials were included in the fitting procedure in order to check the experimental fore-aft symmetry the agreement with the data was not appreciably improved; indeed, the values of the odd-order coefficients were always smaller than the B_2 values and most were zero within their uncertainties. Thus, the measured angular distributions are symmetric about 90° in the center of mass within the statistical accuracy of the data.

In a reaction that produces two identical final particles [such as the ${}^6\text{Li}(d, \alpha)\alpha$ reaction], the measured yield is twice that of a process in which two distinguishable particles are produced in the final state. Hence, it is usual to evaluate the reaction cross section by taking one half of the measured particle yields, and it is these values which are quoted in this report. Unfortunately, it is not always clear in the literature whether the total or one-half the total yields were used in the determination of these cross sections. Figure 5 shows the reaction cross sections obtained in the present experiment ($\sigma = 4\pi B_0$) compared to previous low-energy measurements. The disagreement of about a factor of 2 with the results of Refs. 3 and 7 at energies above 0.5 MeV seem to reflect in part the confusion in the definition of the cross section being reported in these papers. At the lower energies, however, even when this is taken into account, discrepancies still exist (see the dashed curve in Fig. 5 and also Fig. 3). It should be noted that the reaction cross sections of Refs. 6, 7, and 11 are determined from measurements at a single angle only, so that integrated cross-section values are based on the assumption of isotropy of the angular distributions. At deuteron energies < 0.350 MeV this is apparently a rather good assumption (see Table III), and even at higher energies the agreement between the present results and those of Ref. 7 is still good when the data of Ref. 7 are divided by 2.

The ${}^6\text{Li}(d, \alpha)\alpha$ reaction at laboratory deuteron energies between 0.5 and 4.0 MeV has been interpreted by Freeman and Mani¹⁸ in terms of three

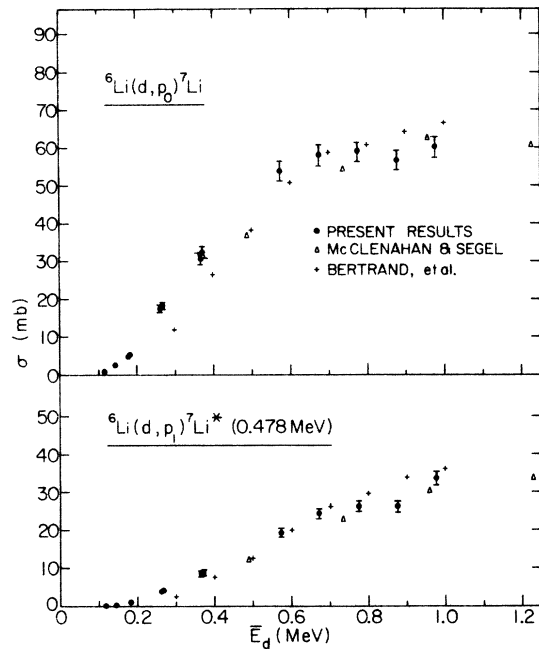


FIG. 8. Total reaction cross sections in the ${}^6\text{Li}(d,p){}^7\text{Li}$ reactions as a function of average deuteron energy, \bar{E}_d . The previous results shown here refer to Refs. 3 and 5 in the text. The relative precision of the present results is indicated by the error bars.

rather broad energy levels in the compound nucleus ${}^8\text{Be}$ at excitation energies of 22.542 (2^+), 24.02 (0^+), and 25.23 (2^+) MeV. Other interpretations of the observed structure in this reaction, as well as in the ${}^7\text{Li}(p,\alpha)\alpha$ and ${}^4\text{He}(\alpha,\alpha){}^4\text{He}$ processes, have also been given.¹⁹ Further discussion based on the results of the present measurements will be presented in a later publication.²⁰

The angular distributions for the ground-state and first-excited-state protons in the ${}^6\text{Li}(d,p){}^7\text{Li}$ reaction and for the corresponding neutrons in the ${}^6\text{Li}(d,n){}^7\text{Be}$ reaction are shown in Figs 6 and 7. The solid curves represent Legendre polynomial fits; the coefficients B_L are presented in Tables IV and V. For the (d,n) reactions, in which measurements were performed at only 7 angles at each deuteron energy, expansion into 6 polynomials was required (except at the lowest energies) to obtain fits with normalized values of χ^2 between ~ 0.5 and ~ 4 , although the fit at 0.873 MeV with 6 polynomials is somewhat poorer. In the case of the (d,p) reactions, good fits (χ^2 values of 0.7–2) were found when the differential cross sections were expanded into a maximum of 7 polynomials, except at 0.975 MeV for the first-excited state reaction at which 11 polynomials were required. The errors used in obtaining the values of χ^2 mentioned here were statistical only.

As observed in Figs. 6 and 7 the data seem to reflect effects of both compound-nucleus and direct-reaction mechanisms. Traditionally, reactions of deuterons with light nuclei have been interpreted²¹ in terms of an incoherent sum of a direct component and a compound contribution estimated on the basis of statistical theories. In the present case, however, a statistical approach is probably unwarranted since the level densities of the nuclei involved are low at the relevant excitation energies. A theoretical approach²² based on a coherent superposition of a direct component determined by a distorted wave Born approximation technique and a compound-nucleus contribution given by an R -matrix description that involves only

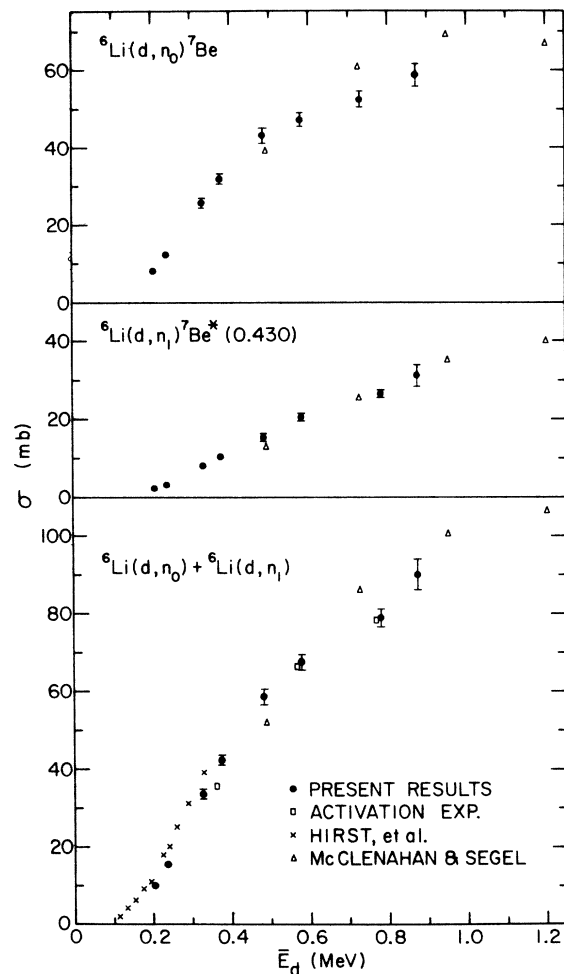


FIG. 9. Total reaction cross sections in the ${}^6\text{Li}(d,n){}^7\text{Be}$ reactions as a function of average deuteron energy, \bar{E}_d . Previous results shown here refer to Refs. 5 and 11. The relative precision of the present results is indicated by the error bars. The open squares represent the results of a supplementary activation experiment. (See text.)

TABLE VI. Differential cross sections (in the laboratory system for the ${}^6\text{Li}(d, p)$ reactions.

E_d (MeV)	$\sigma(\theta_{\text{lab}})$ 90° (mb/sr)																	
	15°	25°	35°	45°	55°	65°	75°	85.5°	97.5°	105°	115°	125°	135°	145°	155°	165°		
	(i) ${}^6\text{Li}(d, p_0){}^7\text{Li}$																	
0.975	7.16	7.44	6.86	6.44	5.05	4.98	4.65	4.14	4.30	4.36	4.11	4.26	4.03	4.41	4.06	3.79 ^a	3.77	
0.875	6.88	6.72	6.38	6.02	5.26	4.73	4.52	3.91	4.19	4.01	3.84	3.84	3.81	3.64	3.78	3.35 ^a	3.56	
0.773	6.69	6.50	6.40	6.24	5.78	5.10	4.81	4.41	4.28	4.17	4.26	4.12	4.04	4.05	3.83	3.65	3.58	
0.673	6.05	6.18	6.27	5.49	5.23	5.00	4.59	4.39	4.34	4.45	4.34	4.13	4.06	3.75	3.89	3.61 ^a	3.55	
0.570	5.26	5.31	5.43	5.13	5.07	4.64	4.51	4.38	4.13	3.98	3.96	3.74	3.62	3.51	3.40	3.15	3.14	
0.369	3.14	3.17	3.17	3.24	2.90	2.86	2.71	2.71	2.51	2.48	2.25	2.24	2.21	2.20	2.10	2.00	1.89	
0.366	3.08	2.90	3.08	2.94	2.74	2.78	2.58	2.47	2.47	2.48	2.25	2.24	2.12	1.88	1.96	1.89	1.87	
0.266	1.72	1.61	1.69	1.65	1.56	1.57	1.45	1.43	1.39	1.41	1.30	1.37	1.25	1.23	1.24	1.14	1.19	
0.263	1.67	1.64	1.64	1.63	1.51	1.59	1.53	1.36	1.36	1.28	1.28	1.29	1.22	1.17	1.17	1.12	1.13	
0.182	0.48	0.48	0.48	0.48	0.49	0.44	0.46	0.42	0.42	0.42	0.42	0.37 ^b	0.40	0.33	0.36	0.33	0.35	
0.179	0.46	0.45	0.45	0.45	0.45	0.45	0.40	0.40	0.40	0.40	0.19	0.36	0.17	0.15	0.15	0.17	0.17	
0.145	0.21	0.22	0.22	0.21	0.19	0.21	0.21	0.21	0.20	0.20	0.19	0.19	0.17	0.17	0.15	0.33	0.32	
0.118	0.073	0.081	0.081	0.081	0.083	0.083	0.083	0.078	0.078	0.078	0.078	0.078	0.067	0.067	0.069	0.069	0.057	
	(ii) ${}^6\text{Li}(d, p_1){}^7\text{Li}^*(0.478 \text{ MeV})$																	
0.975	3.94	4.49	4.71	4.25	3.38	3.16	2.55	2.12	2.24	2.76	2.65	2.29	1.76	1.83	1.70	1.15 ^a	0.86	
0.875	3.20	3.72	3.36	3.41	2.88	2.29	2.02	2.01	2.14	1.97	1.69	1.66	1.30	1.16	1.16	0.96 ^a	0.94	
0.773	2.85	3.00	3.16	3.19	2.83	2.41	2.20	2.04	1.93	1.80	1.81	1.66	1.51	1.40	1.15	0.94	0.87	
0.673	2.73	2.87	3.03	3.13	2.61	2.36	2.06	1.95	1.81	1.79	1.70	1.58	1.40	1.26	1.13	0.84 ^a	0.85	
0.570	1.97	2.25	2.32	2.13	2.12	1.89	1.66	1.61	1.53	1.42	1.37	1.30	1.15	1.01	0.94	0.83	0.72	
0.369	0.85	0.91	0.90	0.94	0.88	0.83	0.78	0.77	0.73	0.69	0.61	0.57	0.56	0.51	0.47	0.43	0.38	
0.366	0.98	0.93	0.92	0.90	0.87	0.84	0.84	0.71	0.71	0.69	0.60	0.58	0.53	0.45	0.45	0.40	0.38	
0.266	0.41	0.40	0.43	0.38	0.41	0.40	0.39	0.38	0.35	0.33	0.32	0.31	0.30	0.26	0.26	0.22	0.22	
0.263	0.41	0.39	0.40	0.42	0.40	0.39	0.37	0.34	0.34	0.33	0.31	0.28	0.26	0.23	0.21	0.19	0.20	
0.182	0.10	0.10	0.10	0.10	0.11	0.11	0.11	0.098	0.098	0.098	0.090	0.077 ^b	0.084	0.070	0.068	0.062	0.064	
0.179	0.10	0.10	0.10	0.10	0.12	0.12	0.10	0.092	0.092	0.092	0.058	0.080	0.037	0.027	0.027	0.064	0.034	
0.145	0.045	0.052	0.052	0.043	0.043	0.043	0.043	0.043	0.045	0.045	0.045	0.045	0.045	0.045	0.045	0.045	0.045	0.045
0.118	0.018	0.016	0.016	0.016	0.015	0.015	0.015	0.016	0.016	0.016	0.016	0.016	0.016	0.016	0.016	0.016	0.016	0.016

^a $\theta_{\text{lab}} = 157^\circ$.^b $\theta_{\text{lab}} = 122^\circ$.

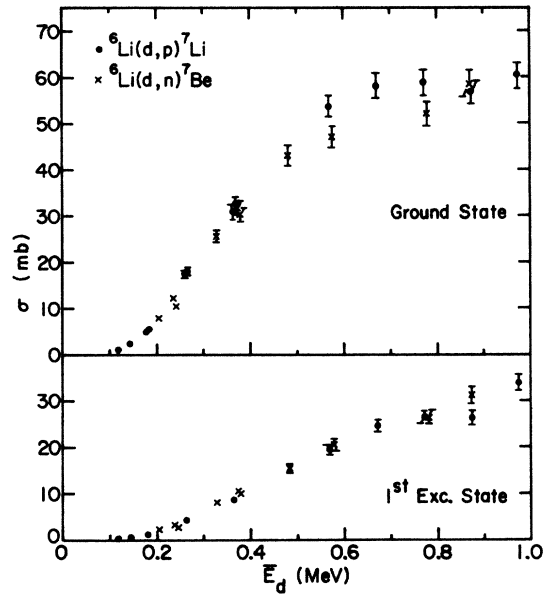


FIG. 10. Comparison of the ${}^6\text{Li}(d,p){}^7\text{Li}$ and ${}^6\text{Li}(d,n){}^7\text{Be}$ total reaction cross sections.

a few nuclear levels in ${}^8\text{Be}$ is being pursued, and the results will be presented in a future report.²⁰

Total reaction cross sections obtained from the coefficient B_0 in the Legendre polynomial expansion of the differential cross section for the ${}^6\text{Li}(d,p){}^7\text{Li}$ and ${}^6\text{Li}(d,n){}^7\text{Be}$ reactions are shown in Figs. 8 and 9 compared with previous low-energy measurements. Also shown in Fig. 9 are the results of an activation experiment in which the total ${}^6\text{Li}(d,n){}^7\text{Be}$ reaction cross section was determined by counting the γ rays from the 0.478-MeV ${}^7\text{Li}$ state formed in the ${}^7\text{Be}$ β decay. The good agreement with the results of the time-of-flight experiment serves as a check on the accuracy of the measured

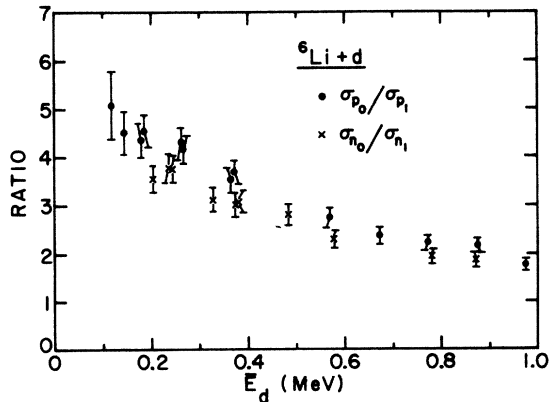


FIG. 11. Ground-to-excited state cross-section ratios for the ${}^6\text{Li}(d,p)$ and ${}^6\text{Li}(d,n)$ reactions as a function of average deuteron energy, \bar{E}_d .

absolute detector efficiencies in the time-of-flight study, and provides additional confirmation of the values of the (d,n) reaction cross sections presented here. In Fig. 10, the reaction cross sections of the (d,p) and (d,n) processes are directly compared.

Since it is expected that the ground- and first-excited states of the mirror nuclei ${}^7\text{Li}$ and ${}^7\text{Be}$ are pure isobaric-spin doublets, the principle of charge symmetry in nuclear reactions would predict that the ${}^6\text{Li}(d,p)$ and ${}^6\text{Li}(d,n)$ reactions to corresponding states have equal intrinsic probability.²³ Although the near equality observed in Fig. 10 is consistent with this principle, it does not constitute a test because of differences in the Coulomb interactions and in phase space. It has been pointed out by Birk *et al.*,²⁴ however, that Coulomb corrections and phase-space effects are almost entirely canceled out by comparing the branching ratios to the ground and first-excited state in the mirror pair. Such quantities are shown in Fig. 11. Although there is a tendency for systematically lower ratios in the (d,n) reaction, charge symmetry is apparently confirmed within the accuracies indicated. This is in agreement with the results of Birk *et al.*²⁴ and Cranberg *et al.*²⁵ in measurements between 0.4 and 3.2 MeV, although the magnitudes of the ratios reported in those references are

TABLE VII. Differential cross sections (in the laboratory system) for the ${}^6\text{Li}(d,n)$ reactions.

\bar{E}_d (MeV)	${}^6\text{Li}(d,n_0){}^7\text{Be}$ $\sigma(\theta_{\text{lab}})$ (mb/sr)						
	0°	30°	60°	75°	111.6°	126.5°	148.5°
0.204	0.72	0.76	0.68	0.63	0.61	0.54	0.56
0.238	1.19	1.18	1.13	0.97	0.92	0.86	0.85
0.328	2.54	2.51 ^a	2.23	2.20	1.74	1.65	1.66 ^b
0.375	3.17	3.13	2.94	2.59	2.25	2.29	2.15
0.482	4.55	4.47 ^a	3.94	3.68	2.93	3.02	2.71 ^b
0.578	4.68	4.87	4.25	3.87	3.42	3.16	2.77
0.779	5.84	6.10	4.76	3.93	3.55	3.46	3.30
0.873	7.47	7.11	4.76	4.34	4.02	4.17	3.86 ^c
\bar{E}_d (MeV)	${}^6\text{Li}(d,n_1){}^7\text{Be}(0.430\text{ MeV})$ $\sigma(\theta_{\text{lab}})$ (mb/sr)						
	0°	30°	60°	75°	111.6°	126.5°	148.5°
0.204	0.20	0.23	0.21	0.22	0.14	0.13	0.13
0.238	0.38	0.37	0.33	0.25	0.24	0.19	0.17
0.328	0.86	0.91 ^a	0.81	0.76	0.51	0.41	0.37 ^b
0.375	1.10	1.16	1.17	0.94	0.70	0.64	0.44
0.482	1.66	1.88 ^a	1.68	1.41	0.89	0.92	0.67 ^b
0.578	2.17	2.65	2.16	1.88	1.21	1.02	0.72
0.779	2.79	3.62	3.11	2.27	1.54	1.28	0.91
0.873	3.35	4.59	3.39	2.88	1.54	1.78	1.21 ^c

^a $\theta_{\text{lab}} = 31^\circ$.

^b $\theta_{\text{lab}} = 147.5^\circ$.

^c $\theta_{\text{lab}} = 149.3^\circ$.

TABLE VIII. Differential cross sections (in the laboratory system) for the ${}^6\text{Li}(d, \alpha)\alpha$ reaction.

\bar{E}_d (MeV)	$\sigma(\theta_{\text{lab}})$ (mb/sr)							
	15°	25°	35°	45°	55°	65°	75°	82.5°
0.975	3.31	3.13	2.67	2.39	2.01	2.01	1.96	1.74
0.875	3.52	3.14	2.77	2.56	2.32	2.18	2.09	1.86
0.773	3.31	3.06	2.98	2.86	2.62	2.38	2.32	2.16
0.673	3.41	3.30	2.96	2.85	2.65	2.55	2.46	2.26
0.570	3.08	3.07	2.95	2.80	2.74	2.55	2.45	2.36
0.369	2.06	2.07	2.08	2.05	1.91	1.90	1.83	1.76
0.366	2.04	2.03	2.01	1.95	1.82	1.86	1.80	
0.266	1.29	1.22	1.27	1.20	1.21	1.18	1.13	1.11
0.263	1.28	1.28	1.20	1.24	1.16	1.16	1.13	
0.182	0.38		0.36		0.36	0.35	0.34	
0.179	0.36		0.34		0.33		0.33	
0.145	0.17		0.17		0.17		0.17	
0.118	0.065		0.065		0.068			

\bar{E}_d (MeV)	$\sigma(\theta_{\text{lab}})$ (mb/sr)								
	90°	97.5°	105°	115°	125°	135°	145°	155°	165°
0.975	1.86	1.83	1.75	1.84	1.80	2.10	2.06	2.22 ^a	2.22
0.875	2.03	2.00	1.83	1.99	2.01	2.05	2.17	2.28 ^a	2.31
0.773	2.16	2.11	2.12	2.11	2.15	2.22	2.20	2.24	2.33
0.673	2.28	2.38	2.39	2.29	2.33	2.32	2.30	2.30 ^a	2.51
0.570	2.36	2.28	2.32	2.31	2.32	2.27	2.33	2.28	2.32
0.369	1.72	1.71	1.71	1.64	1.65	1.69	1.66	1.60	1.59
0.366	1.70		1.65	1.63	1.56	1.55	1.58	1.56	1.56
0.266	1.08	1.07	1.06	1.07	1.03	1.03	1.05	0.97	1.04
0.263	1.05		1.10	1.06	1.03	1.02	1.04	1.01	0.98
0.182	0.34		0.32	0.32 ^b	0.32		0.30		0.30
0.179	0.32			0.30		0.29		0.29	0.28
0.145	0.16		0.16		0.15		0.16		0.14
0.118	0.065				0.057		0.058		0.049

^a = 157°.^b = 122°.

somewhat higher than the present results in the region of overlap.

We wish to thank R. Amrein and the operating staff of the Dynamitron accelerator for their cooperation in performing the measurements reported here.

APPENDIX

The experimental laboratory differential cross sections at the average lab energies \bar{E}_d for the

${}^6\text{Li}(d, p)$, ${}^6\text{Li}(d, n)$, and ${}^6\text{Li}(d, \alpha)$ reactions are given in Tables VI, VII, and VIII following. Differential cross sections in the center-of-mass system can be obtained from the coefficients B_L given in Tables III, IV, and V by use of the expansion

$$\sigma_{\text{c.m.}}(\theta_{\text{c.m.}}) = \sum_L B_L P_L(\cos\theta_{\text{c.m.}}),$$

where $P_L(\cos\theta)$ are the Legendre polynomials as given, for example, by Jahnke and Emde.²⁶

†Work supported by the U. S. ERDA, Division of Physical Research.

¹V. A. Crocker, S. Blow, and C. J. H. Watson, Culham Lab. Report No. CLM-P240, 1970 (unpublished); J. R. McNally, Jr., USAEC Report No. ORNL-TM-4647, 1974 (unpublished); J. R. McNally, Jr., USAEC Report No. ORNL-TM-4575, 1974 (unpublished); J. R.

McNally, Jr., in *Proceedings of the Conference on Nuclear Cross Sections and Technology*, NBS Special Publication No. 425 (National Bureau of Standards, Washington, D.C., 1975), Vol. I, p. 683.

²See, for example, W. A. Fowler, G. R. Caughlan, B. A. Zimmerman, *Ann. Rev. Astron. Astrophys.* **13**, 69 (1975).

- ³F. Bertrand, G. Greiner, and J. Poirer, Centre d'Etudes de Lineil Report No. CEA-R-3428, 1968 (unpublished).
- ⁴G. Bruno, J. Decharge, A. Perrin, G. Surget, and C. Thibault, *J. Phys.* **27**, 517 (1966).
- ⁵C. R. McClenahan and R. E. Segel, *Phys. Rev. C* **11**, 370 (1975).
- ⁶G. A. Sawyer and J. A. Phillips, Los Alamos Scientific Laboratory Report No. LA-1578, 1953 (unpublished).
- ⁷W. Whaling and T. W. Bonner, *Phys. Rev.* **79**, 258 (1950).
- ⁸R. L. Macklin and H. E. Banta, *Phys. Rev.* **97**, 753 (1955).
- ⁹C. C. Lee, *J. Korean Phys. Soc.* **2**, 1 (1969).
- ¹⁰J. M. F. Jeronimo, G. S. Mani, F. Picard, and A. Sadeghi, *Nucl. Phys.* **38**, 11 (1962).
- ¹¹F. Hirst, I. Johnstone, and M. J. Poole, *Philos. Mag.* **45**, 762 (1954).
- ¹²A. J. Elwyn, R. E. Holland, F. J. Lynch, J. E. Monahan, and F. P. Mooring, in *Proceedings of the Conference on Nuclear Cross Sections and Technology*, NBS Special Publication No. 425 (National Bureau of Standards, Washington, D.C., 1975), Vol. I, p. 692; A. J. Elwyn, R. E. Holland, J. E. Monahan, C. N. Davids, L. Meyer-Schützmeister, F. J. Lynch, and F. P. Mooring, *Proceedings of the IV Conference on Small Accelerators* (IEEE, New York, N.Y., 1976), p. 262.
- ¹³A. J. Elwyn, R. E. Holland, C. Davids, F. J. Lynch, J. E. Monahan, L. Meyer-Schützmeister, and F. P. Mooring (unpublished).
- ¹⁴A. J. Elwyn, J. E. Monahan, and F. J. D. Serduke, *Nucl. Sci. Engin.* **63**, 343 (1977).
- ¹⁵See, for example, C. Williamson, J. P. Boujot, and J. Picard, Centre d'Etudes Nucleaire de Saclay, Report No. CEA-R-3042, 1966 (unpublished); J. F. Janni, Air Force Weapons Laboratory Report No. AFWL-TR-65-150, 1966 (unpublished); J. F. Ziegler and W. K. Chu, *At. Data Nucl. Data Tables* **13**, 463 (1974).
- ¹⁶We thank Dr. F. J. D. Serduke for computational assistance with the calculations of average deuteron energies.
- ¹⁷The target chamber 0° position was periodically checked by measuring the Rutherford scattering cross section of 1-MeV α particles from Au with a single detector that could be moved to various forward angles on both sides of the incident deuteron beam.
- ¹⁸R. M. Freeman and G. S. Mani, *Proc. Phys. Soc. (London)* **85**, 267 (1965).
- ¹⁹See, for example, Tsan Ung Chan, J. P. Longequeue, and H. Beaumevielle, *Nucl. Phys.* **A124**, 449 (1969); N. Kumar and F. C. Barker, *ibid.* **A167**, 434 (1971); A. D. Bacher, F. G. Resmini, H. E. Conzett, R. de Swinarski, H. Meiner, and J. Ernst, *Phys. Rev. Lett.* **29**, 1331 (1972).
- ²⁰J. E. Monahan and A. J. Elwyn (unpublished).
- ²¹See, for example, D. L. Powell, G. M. Crawley, B. V. N. Rao, and B. A. Robson, *Nucl. Phys.* **A147**, 65 (1970); H. Cords, G. U. Din, and B. A. Robson, *ibid.* **A127**, 95 (1969).
- ²²R. G. Thomas, *Phys. Rev.* **100**, 25 (1955).
- ²³D. H. Wilkinson, *Philos. Mag.* **2**, 83 (1957).
- ²⁴M. Birk, G. Goldring, P. Hillman, and R. Moreh, *Nucl. Phys.* **41**, 58 (1963).
- ²⁵L. Cranberg, A. Jacquot, and H. Liskien, *Nucl. Phys.* **42**, 608 (1963).
- ²⁶E. Jahnke and F. Emde, *Tables of Functions* (Dover, New York, 1945), 4th ed., p. 107.